Journal of Environment and Sustainable Mining Vol.1 No.1 (2025) 1-21

Journal of Environment and Sustainable Mining

Which one controls the absorption of DR 80 and DR 81 dyes by diatomite? Transport of pollutant in pores or adsorption on surfaces

Faramarz Doulati Ardejani[1*], **Khashaiar Badii**[2]

[1] School of Mining Engineering, College of Engineering, University of Tehran, Tehran, Iran.
[2] School of Engineering, Deakin University, Waurn Ponds, VIC 3216, Australia.

ARTICLE INFO

Article type:
Research Article

Article history:
Received: 2025-01-02
Received in revised form: 2025-02-27
Accepted: 2025-03-22
Available online: 2025-03-29

Keywords:
Adsorption,
Diatomite,
Adsorption steps,
Diffusion through pores,
Adsorption on surfaces.

ABSTRACT

The adsorption steps of Direct Red 80 (DR 80) and Direct Red 81 (DR 81) dyes from a synthetic aqueous solution were investigated using diatomite as a low-cost, abundant, and naturally available adsorbent. The equilibrium and kinetics studies were first carried out. The effects of pH, contact time, temperature, initial concentration, calcinations, and sorbent dose on the adsorption process were studied in order to obtain the maximum dyes removal. The highest adsorption was obtained at pH 2. The maximum adsorption of DR 80 and DR 81 dyes onto diatomite was 90.19% and 93.08 % respectively. It was further found that both investigated steps of adsorption, including diffusion and adsorption on surfaces, are important. However, the size of the dye molecule is more effective, especially on the adsorption capacity. It means that diffusion through the micro-pores is the most important step of the adsorption mechanism, and adsorption on the adsorbent surfaces has the second place of significance.

Cite this article: Doulati Arde Jani, F. and Badii, K. (2025). Which Controls the Absorption of DR 80 and DR 81 Dyes by Diatomite? Transport of Pollutant in Pores or Adsorption on Surfaces. *Journal of Environment and Sustainable Mining*, 1(1), 1-21. https//doi.org/10.22111/jesm.2023.44152.1002

Publisher: University of Sistan and Baluchestan.
DOI: https//doi.org/10.22111/jesm.2023.44152.1002

* Corresponding author: **Faramarz Doulati Ardejani**
E-mail address: fdoulati@ut.ac.ir

1 .Introduction

Textile industries often produce huge amounts of polluted effluents. The environmental problem associated with such effluents is a major concern for public health. Synthetic dyes, suspended solids, and dissolved organics are the main hazardous materials found in textile effluents [1].

These materials can significantly affect the physical and chemical properties of fresh water. In addition to the undesirable colours of textile effluents, some dyes may degrade to produce carcinogens and toxic products [2]. Furthermore, the coloured effluents reduce light penetration and potentially prevent photosynthesis [3, 4].

Several treatment plans have been proposed for the removal of synthetic dyes from aqueous solutions. Coagulation [5], flocculation [6], photocatalytic degradation [7-9], membrane filtration [10], microbiological decomposition [11], electrochemical oxidation [12], fungus biosorbent [13], and adsorption [2-5, 14-20] are the most commonly used methods for dyes removal from the waste effluent systems.

Adsorption is considered to be a particularly competitive, economically cost-effective, and efficient process for the removal of dyes, heavy metals, and other organic and inorganic hazardous impurities from aqueous solutions [21-23]. Besides that, the microbiological, photocatalytic, and electrochemical decomposition methods are not efficient because many dyes cannot be easily decomposed [12].

Activated carbon is the most efficient and popular adsorbent and has been used with great success. However, the high cost of activated carbon sometimes restricts its applicability for dye removal [16, 22, 24]. Therefore, in recent years, considerable attention has been devoted to the study of different types of low-cost and efficient materials as sorbent for dyes removal from the aqueous solutions, which included wood and saw dust [25, 26], fly ash [27], wheat straw [28], apple pomace [28], orange peel [29, 30], banana peel [31], peanut hull [3], leaf [32], almond shells [14], red mud [18] etc.

Many attempts have been made by numerous researchers to investigate the use of diatomite as an adsorbent for removing some contaminants such as toxic metals [33], basic dye (Methylene blue) [2], basic and reactive dyes (Methylene blue, reactive black, reactive yellow) [4, 34], some textile dyes (Sif Blau BRF, Everzol Brill Red 3BS, Int Yellow 5GF) [35] and acidic dye (Acid blue 25) [36]. However, the adsorption mechanisms of pollutants by diatomite as an adsorbent have not been greatly investigated.

Diatomite is a pale-coloured, soft, lightweight siliceous sedimentary rock made up principally from the skeletons of aquatic plants called diatoms. Diatomite contains a wide variety of shapes and sizes of diatoms, typically 10-200, in a structure including up to 80-90 % pore spaces [33]. Due to the extremely porous structure, low density, and high surface area of diatomite, there is a possibility to use it for the adsorption of organic and inorganic chemicals. Furthermore, these unique properties caused its applications as filtration media in a number of industries [33, 35]. It has been suggested that diatomite can be successfully used as a cost-effective alternative to activated carbon. Diatomite is approximately 500 times cheaper than commercial activated carbon [35]. Diatomite is found in abundance in Iran.

When the adsorption mechanism is discussed, most researchers would think about the last step of this process and the procedure in which a pollutant connects to the adsorbent surfaces. It is not clear which part of an adsorption mechanism is the bottle–neck of this process. The formal mechanism of pollutant adsorption has been widely discussed in many scientific texts. The pollutants would transfer in agitated fluid bulk (first step) and pass through the interface between fluid and solid (second step). In the third step, the pollutants would enter the pores and transfer to the adsorption sites. The last step of the process is the adsorption of pollutants on the surfaces of adsorbent [6, 29, 34, 37, 38]. If the agitation is enough, the first and second steps cannot control the whole process, but mass transfer inside the pores and adsorption on the adsorbent surfaces can control the process. Most investigations paid no attention to the third step of the adsorption process.

This paper describes a study of the mechanisms of dye adsorption on diatomite and, most importantly, indicates the bottle-neck of the process. As a typical investigation, the possibility of utilization of diatomite was checked as an adsorbent for the removal of DR 80 and DR 81 dyes from an aqueous solution. These two dyes were selected because their structures are similar. However, the size of DR 81 is half that of DR

80. The raw and calcined diatomite samples were compared due to their different microscopic structures. The equilibrium and kinetic studies were carried out to observe the effects of various process parameters such as pH, contact time, initial dye concentration, temperature, calcinations, and the sorbent dose on the adsorption process. Equilibrium data were fitted to the various adsorption isotherms, including Langmuir, Freundlich, and Brunauer-Emmett-Teller (BET) isotherms, to select an appropriate isotherm model. Moreover, a kinetics study of the adsorption process was also considered to describe the rate of sorption.

The literature review thus far has indicated that the adsorption mechanisms of the DR 80 and DR 81dyes on diatomite have not been studied. Investigation into the mechanism through which the adsorption takes place is an important matter for developing a treatment system based on the adsorption process. Therefore, the main objective of this paper was to study the above mechanism.

2. Experimental

2.1. Adsorbent preparation

DR 80 and DR 81 dyes were obtained from Ciba Ltd. and used without further purification. The chemical structures of these dyes are shown in Fig. 1. It is clear that the structures of these colorants are similar, but the molecular size of DR 80 (molecular weight and size are 1373.05 and 10.73 Å) is two times greater than that of DR81 (molecular weight and size are 675.60) [39].

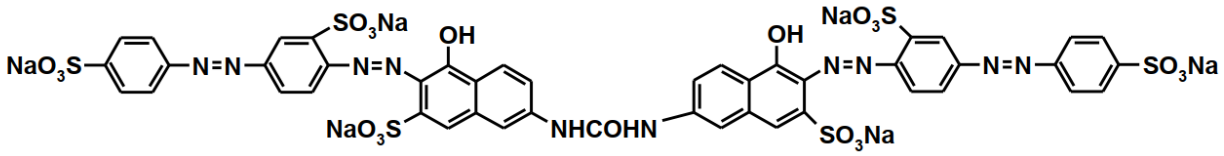

(a) DR 80 dye

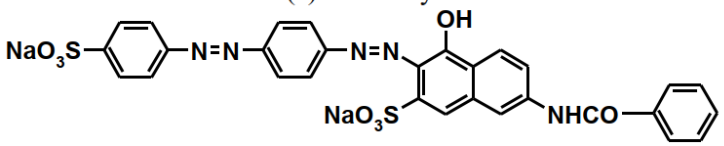

(b) DR 81 dye

Fig. 1. Chemical structures of DR 80 and DR 81 dyes used in this study.

Distilled water was employed throughout as a solvent. For adsorption experiments, various concentrations of dye solutions (50, 100, and 150 mg/L) were prepared. The pH measurements were conducted using a Hach pH meter. The pH adjustments of the solution were made by adding a small amount of HCl or NaOH (1M). These chemicals were of analytical grade and purchased from Merck, Germany.

2.3. Adsorption procedure

The adsorption measurements were performed by mixing various amounts of diatomite (0.2 –1.1 g) in the jars containing 250 mL of dye solutions with varying concentrations (varied from 50 to 150 mg/L) and 5 g NaCl at various pHs (2-12). pH studies were carried out to determine the optimum pH at which the maximum dye removal could be achieved with diatomite. Adsorption experiments were conducted at various concentrations of dye solutions (50, 100, and 150 mg/L), using an optimum amount of diatomite (0.9 g) at pH 2, an agitation speed of 200 rpm, and a temperature of 25 °C for 5 hours to attain equilibrium conditions.

An FC6S-VELP (Scientifica) jar test was used for agitating purposes. The changes of absorbance were determined at certain time intervals (2, 4, 6, 8, 10, 20, 30, 60, 120, 180, 240, 300, and 1440 minutes) during the adsorption process. After adsorption experiments, the dye solutions were centrifuged for 12 minutes in a Hettich EBA20 centrifuge at 4000 rpm in order to separate the sorbent from the solution, and the dye

concentration was finally determined. For isotherm studies, the results were fitted to the various adsorption isotherm models incorporating Langmuir, Freundlich and Brunauer Emmett-Teller (BET) isotherms.

2.4. Analysis of the samples

The residual dye concentrations in the aqueous medium were determined using a CECIL 2021 spectrophotometer corresponding to the maximum wavelength (max) of DR 80 and DR 81 dyes (542.5 and 508 nm, respectively).

3. Results and discussion

3.1. Surface characterization

In order to explore the surface characteristics of diatomite, an FTIR analysis was performed in the range of 450 to 4000 cm-1. Fig. 2 shows the infra-red spectra of RD.

The peak positions showing major adsorption bands were observed at 3436.26, 1637.30, 1087.19, 796.25, 625.43, 526.76, and 471.65 cm-1. The band at 3436.26 cm-1 is due to the free silanol group (Si-O-H), the band at 1637.30 cm-1 represents H-O-H bending vibration of water, the band at 1087.19 cm-1 reflects the siloxane (-Si-O-Si-) group stretching, the bands at 796.25 cm-1 and 625.43 cm-1 correspond to SiO-H vibration. The peak positions of 526.76 cm-1 and 471.65 cm-1 are attributed to the Si-O-Si bending vibration.

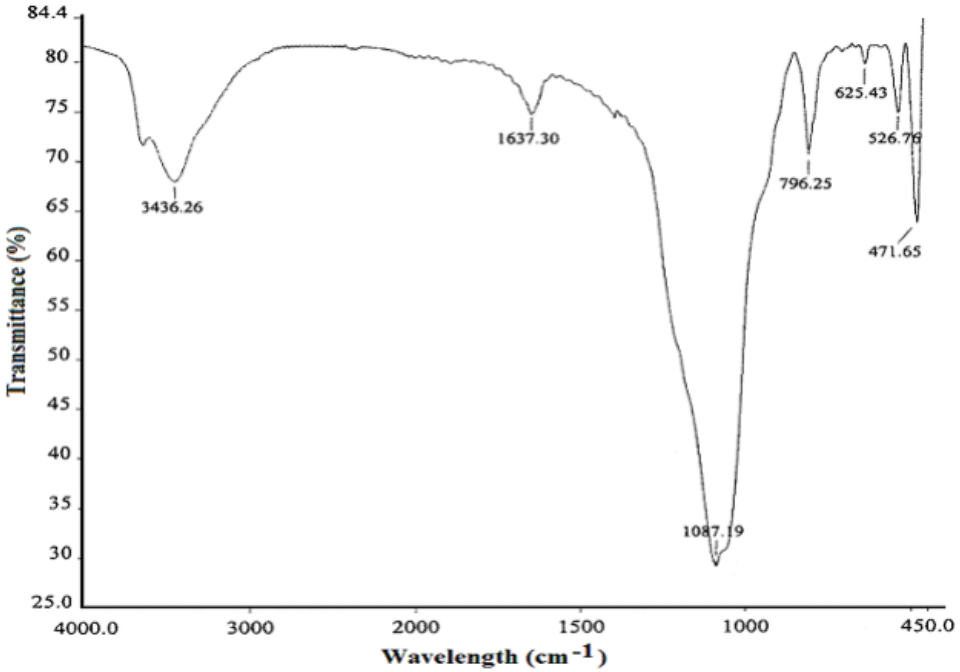

Fig 2. Fourier transforms infra-red spectra of RD.

Scanning electron microscopic (SEM) of both RD and CD was carried out using a LEO 1455VP scanning microscope before and after the adsorption process. SEM is noted to be a primary tool for the investigation of the surface characteristics and the fundamental physical properties of the adsorbent. Furthermore, it can be successfully used to determine the particle shape, pore spaces, and proper size distribution of the adsorbent. Scanning electron micrographs of RD and CD obtained before adsorption are shown in Fig. 3. In addition, Figs. 4 and 5 show SEM micrographs of RD and CD obtained after the adsorption experiments, respectively. As illustrated well in Fig. 3a, diatomite originally has considerable numbers of pore spaces where dyes can be adsorbed into these relatively large pores. An important change

in the surface characteristics and the size of the pore spaces of the diatomite was obtained after the calcination process at 980˚C. As it is evident from Fig. 3b, the thermal treatment of the diatomite reduced the volume of the pore spaces and removed the surface functional groups from the RD. Moreover, the solid structure of diatomite became more visible. Fig. 4 shows that the DR 80 and DR 81 dyes were homogeneously adsorbed and trapped in the pore spaces of the RD. Fig 5 shows the SEM of CD after the adsorption of DR 80 and DR 81 dyes. Due to the thermal process of diatomite, the removal of these dyes from aqueous solution decreased.

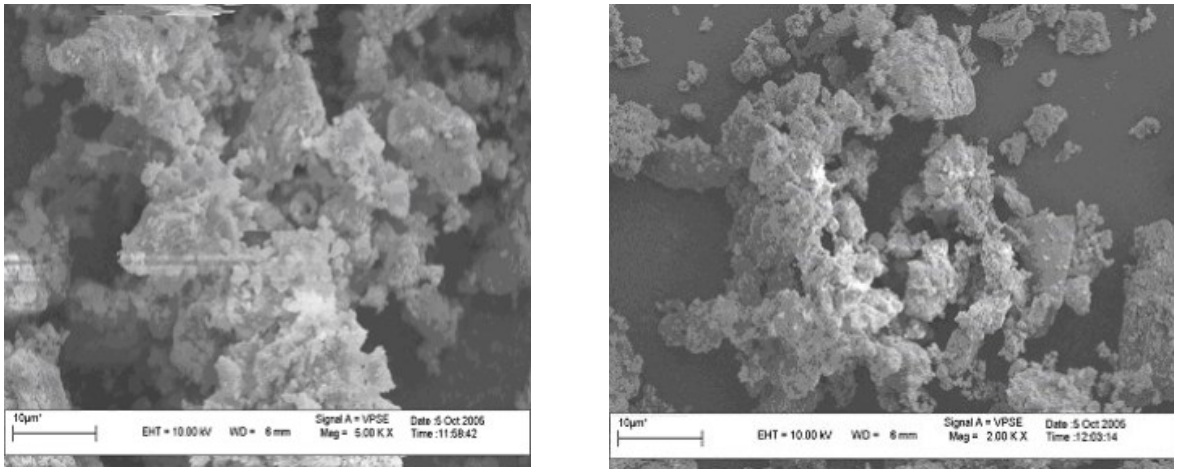

(a) RD **(b) CD**

Fig. 3. Scanning electron micrographs of (a) RD before adsorption, (b) CD before adsorption.

In order to determine the compositions of RD and CD, XRD analysis was performed using a Philips Xpert x-ray diffractometer and the sample was scanned from 10º to 70º. XRD results of the RD and CD are illustrated in Fig. 6. It can be seen from Fig. 6 that the x-ray pattern of the RD is different from the pattern of the CD, suggesting that a phase transformation probably occurred during the calcination process. The main composition of RD is quartz, anorthite and muscovite. It is evident that sanidine appeared while anorthite and muscovite were completely removed as the diatomite was calcined at 980˚C. In fact, some peaks in the diatomite disappeared and some peaks were created by the thermal process. Similar behaviour was previously investigated by other researchers [4].

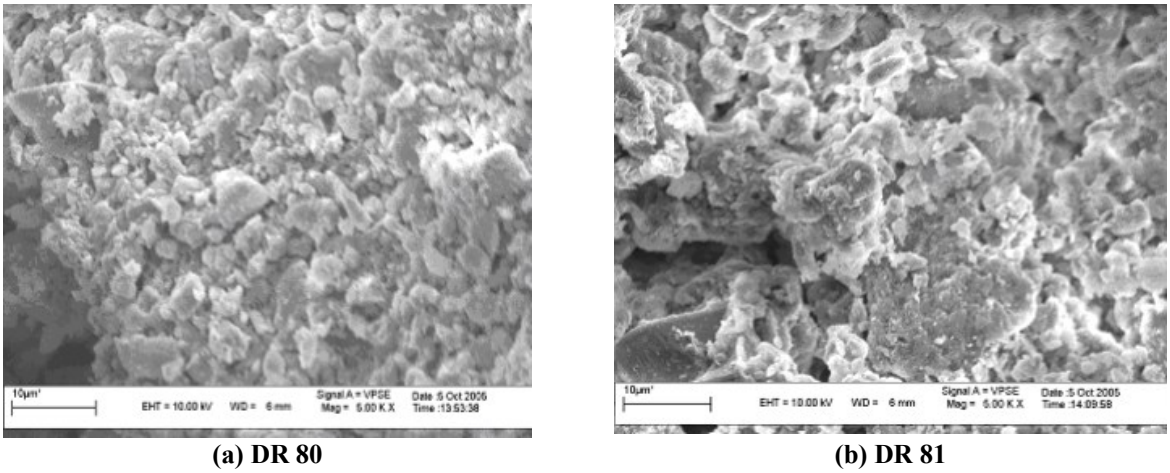

(a) DR 80 **(b) DR 81**

Fig. 4. Scanning electron micrographs of (a) RD after adsorption of DR 80 dye (b) RD after adsorption of DR 81 dye; Conditions: adsorbent dosage = 1.1 g for DR 80 and 0.5 g for DR 81, T= 25 0C , equilibrium time = 5 hours, agitation speed = 200 rpm.

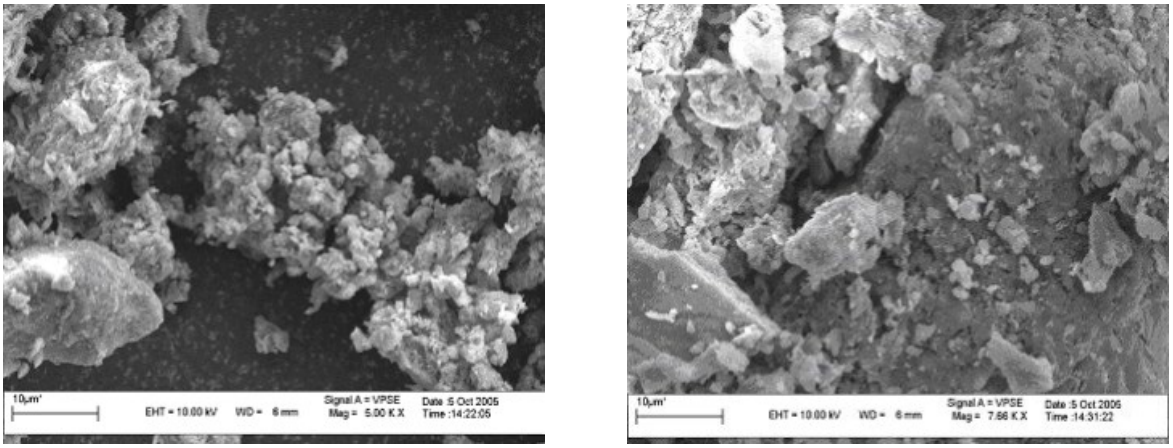

(a) DR 80 **(b) DR 81**

Fig. 5. Scanning electron micrographs of (a) CD after adsorption of DR 80 dye and (b) CD after adsorption of DR 81 dye; Conditions: adsorbent dosage = 1.1 g for DR 80 and 0.5 g for DR 81, T= 25 0C , equilibrium time = 5 hours, agitation speed = 200 rpm.

In order to determine the compositions of RD and CD, XRD analysis was performed using a Philips Xpert x-ray diffractometer and the sample was scanned from 10º to 70º. XRD results of the RD and CD are illustrated in Fig 6. It can be seen from Fig 6 that the x-ray pattern of the RD is different from the pattern of the CD, suggesting that a phase transformation probably occurred during the calcination process. The main composition of RD is quartz, anorthite and muscovite. It is evident that sanidine was appeared while anorthite and muscovite were completely removed as the diatomite was calcined at 980˚C. In fact, some peaks in the diatomite disappeared and some peaks were created by the thermal process. Similar behaviour was previously investigated by other researchers [4].

In addition, the specific surface area of the diatomite was determined by BET method. In this investigation,

the values 129.384 m2/g and 7.458 m2/g were calculated for RD and CD, respectively. The amount of the specific surface area was reduced more than 17 times after the calcination process and it should not be ignored. A particle size analysis was carried out to determine the distribution of particles of the adsorbent. As Fig. 7 shows, the maximum distribution of particles is varied from 10 to 40 µm.

3.2. Effect of adsorbent dose

The effect of adsorbent dose on the percentage removal of DR 80 and DR 81 dyes from aqueous solution was studied by contacting 250 mL of dye solution with an initial dye concentration of 50 mg/L at 25 ˚C. Various amounts of RD and CD (0.2-1.1 g for DR 80 and 0.1-0.7 g for DR 81) were used. Fig 8 shows the percentage removal of DR 80 and DR 81 dyes versus adsorbent concentrations. In general, the percentage removal of dyes increased as the sorbent concentration was increased over the sorbent range mentioned above. As it is depicted in Fig 8, the percentage removal of DR 80 dye increased from 17.5 to 87.16 % and from 15 to 29.45 % for RD and CD, respectively. Furthermore, for the adsorption of DR 81 dye on RD, the percentage removal increased from 31.45 to 93.18 % while the sorbent dose was increased from 0.1 to 0.5 g. After that, it decreased to 75.62 % as the adsorbent dose was raised from 0.5 to 0.7 g. Within the range 0.1-0.7 g, the percentage removal of DR 81 dye by CD did not change considerably. It increased from 20.92 to 25.05 % (for an adsorbent range 0.1-0.5 g) and then decreased to 23.24 %. Based on the results shown in Fig 8, 1.1 and 0.5 g of diatomite were used for further experiments with DR 80 and DR 81 dyes, respectively.

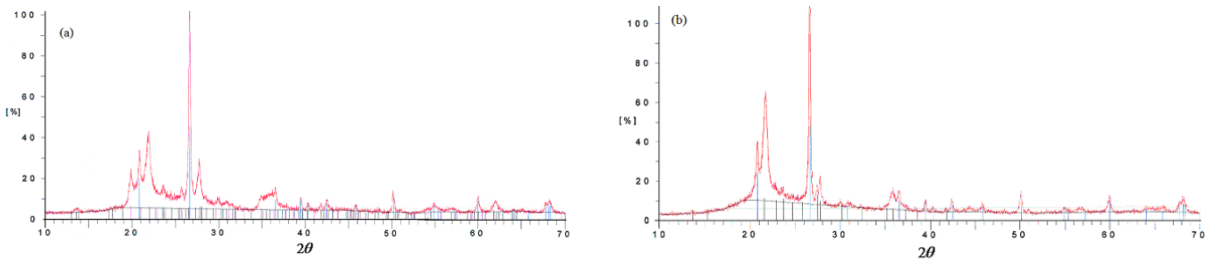

Fig. 6. XRD patterns of (a) RD and (b) CD.

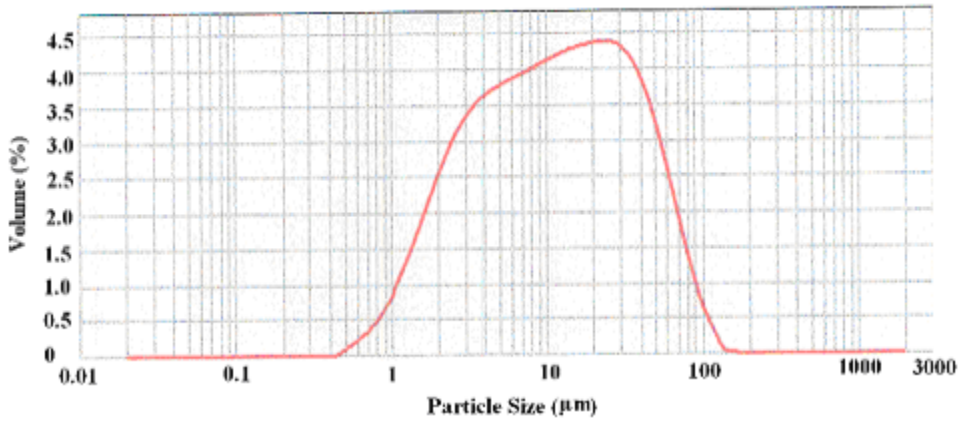

Fig. 7. Particle size analysis of diatomite.

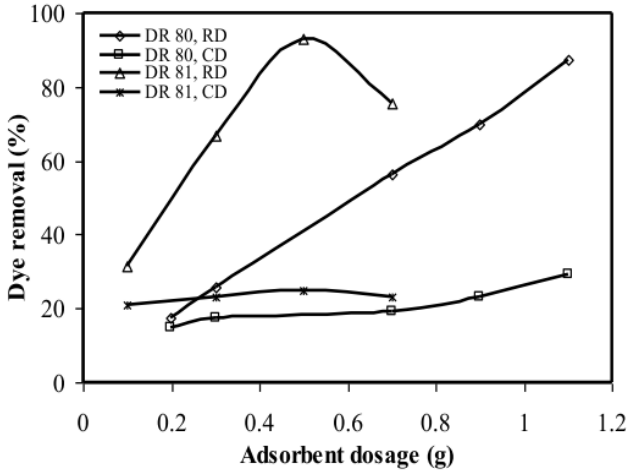

Fig. 8. Effect of adsorbent dosage on the percentage removal of DR 80 and DR 81 dyes by RD and CD; Conditions: T= 250C , initial dye concentration = 50 mg/L, pH = 2, agitation speed = 200 rpm.

3.3. Effect of initial dye concentration

Effect of initial dye concentration on the adsorption of DR 80 and DR 81 dyes by RD and CD adsorbents are illustrated in Fig. 9. As it is obvious from this Fig, for RD adsorbent, the percentage removals ecreased from 90.19 to 40.91% and from 93.08 to 44.59 % for DR 80 and DR 81 dyes respectively as dye concentration increased from 50 to 150 mg/L. Moreover, using CD adsorbent, the adsorption of DR 80 and DR 81 dyes decreased from 14 to 9.06 % and 27.8 to 16.2 % as the initial dye concentration increased from 50

to 150 mg/L.

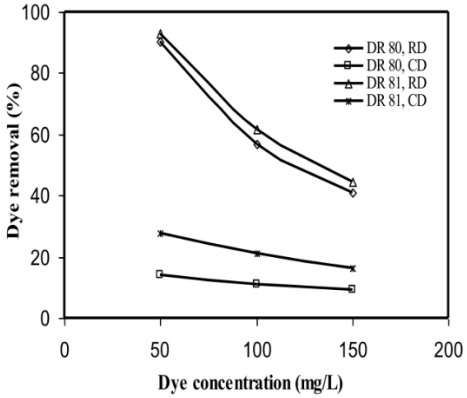

Fig. 9. Effect of initial dye concentration on adsorption of DR 80 and DR 81 dyes by RD and CD; Conditions: contact time= 300 minutes, T= 250C , pH = 2, agitation speed = 200 rpm.

3.4. Effect of contact time

The adsorption of DR 80 and DR 81 dyes was studied as a function of contact time. Figs 10 and 11 show the effect of contact time on the percentage removal of DR 80 and DR 81 dyes from an aqueous system by RD. The initial dye concentration was varied from 50 to 150 mg/L. The rate of dye adsorption was rapid in the initial stages of the adsorption process. It gradually decreased with time until equilibrium. As it is evident from Fig 10, after 2 minutes of the adsorption process, the amounts of DR 80 dye adsorption by RD reached to 75.70, 41.32 and 30.12 % for initial dye concentrations of 50, 100 and 150 mg/L, respectively. Furthermore, Fig 11 shows that after the same contact time (2 min), the percentage removals of 61.78, 47.30 and 41.30 % were obtained for DR 81 dye by RD as dye concentrations increased from 50 to 150 mg/L.

3.5. Effect of calcination process

A thermal treatment (calcination process) was also performed on RD at 980 ˚C. This process has two major effects on RD, as it is well documented by Khraisheh et al. [4]. (a) As shown in Fig 12, when diatomite is heated at high temperature, the surface functional groups on the diatomite surface (-OH groups) are removed. The removal of OH groups has a negative effect on the adsorption process. (b) The second important effect of the calcination process is the change in the volume and size of the pore spaces, and especially the specific surface area of the adsorbent, which was originally found on the surfaces of diatomite. As a result, these changes may have a significant effect on the percentage removal of dyes from aqueous solution.

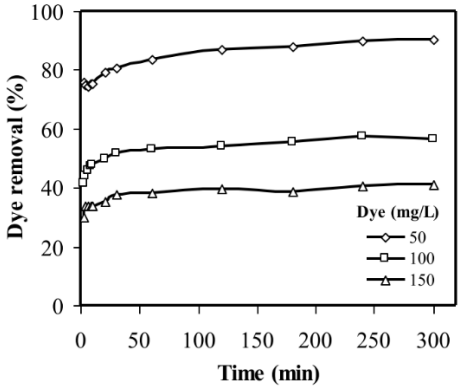

Fig. 10. Effect of contact time on adsorption of DR 80 dye on RD; Conditions: T= 25 0C , pH = 2, agitation speed = 200 rpm, adsorbent dosage = 0.9 g.

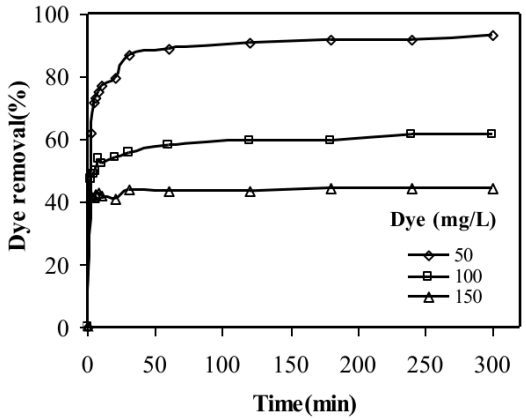

Fig. 11. Effect of contact time on adsorption of DR 81 dye on RD; Conditions: T=25 0C , pH = 2, agitation speed = 200 rpm, adsorbent dosage = 0.9 g.

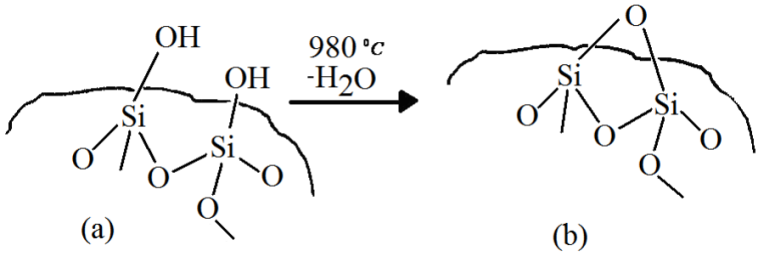

Fig. 12. Schematic representation of calcination process at 980 ˚C [4], a) Molecular structure of diatomite before heating, b) Molecular structure of diatomite after heating.

Figs. 13 and 14 show the effect of contact time and initial dye concentration on the adsorption of DR 80 and DR 81 dyes by CD. As illustrated well, the dye removal rate is fast at the early stages of the adsorption process. Comparison of the Figs. 10 and 11 with Figs. 13 and 14 show that a considerable reduction was obtained in the adsorption of DR 80 and DR 81 dyes by thermal treatment of diatomite at 980˚C. Moreover, the specific surface area was reduced by more than 17 times after the calcination process.

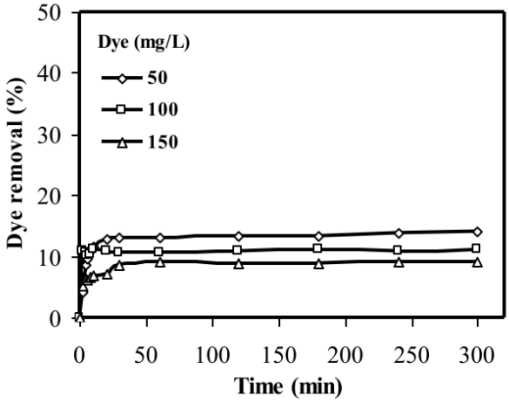

Fig. 13. Effect of contact time and dye concentration on adsorption of DR 80 dye on CD; Conditions: T= 250C , pH = 2, agitation speed = 200 rpm, adsorbent dosage = 0.9 g.

3.6. Effect of molecular size

As explained in section (2.2), the molecular size of DR 80 is two times greater than that of DR 81. It means that DR 80 dye needs more spaces and a bigger pore size to reach the adsorption sites and its adsorption is therefore slower. Comparison of the adsorption process in Figs 8-11 and 13-16 confirms this fact. Furthermore, the adsorption capacity of diatomite is lower for DR 80 than that of DR 81, as expected.

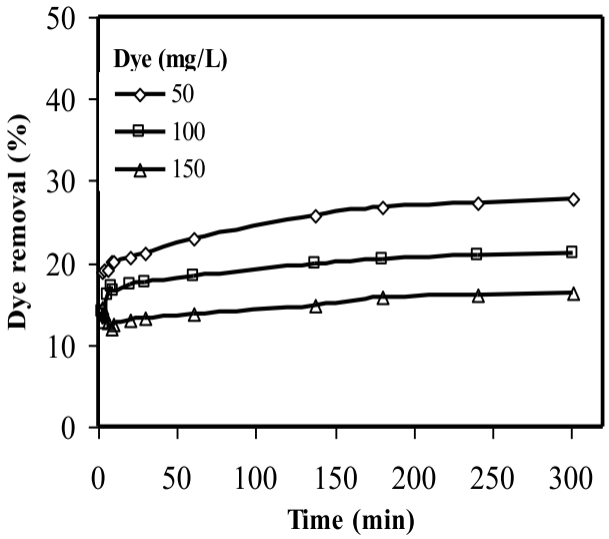

Fig. 14. Effect of contact time and dye concentration on adsorption of DR 81 dye on CD; Conditions: T= 250C , pH = 2, agitation speed = 200 rpm, adsorbent dosage = 0.9 g.

3.6. Adsorption isotherms

In adsorption studies, it is necessary to determine isotherm models describing the relationships between equilibrium concentrations of dye in the adsorbent particles, q , and in the aqueous phase, C , at a given temperature. Adsorption isotherms of DR 80 and DR 81 dyes onto both RD and CD are shown in Fig 15. It can be seen from Fig 15 that the amounts of adsorbed DR 80 and DR 81 dyes on RD were much higher than that of CD. RD showed the highest adsorption capacity for the removal of DR 81 than that of DR 80. In this study, the experimental data were evaluated by various isotherm models including Langmuir, Freundlich [5, 13, 16, 40, 41] and Brunauer-Emmett-Teller (BET) [13, 42] isotherms.

One of the most common isotherm models is the Langmuir model. It is applicable for monolayer adsorption on a surface containing a finite number of identical adsorption sites [16]. A linear expression for the Langmuir isotherm can be expressed as:

$$1/q_e = \left(\frac{1}{K_L Q_0}\right)(1/C_e) + 1/Q_0 \quad (1)$$

Where, Ce is the concentration of dye under equilibrium conditions (mg/L), qe denotes the amount of dye adsorbed at equilibrium (mg/g), Q0 indicates the maximum adsorption capacity and KL represents the Langmuir isotherm constant (l/mg).

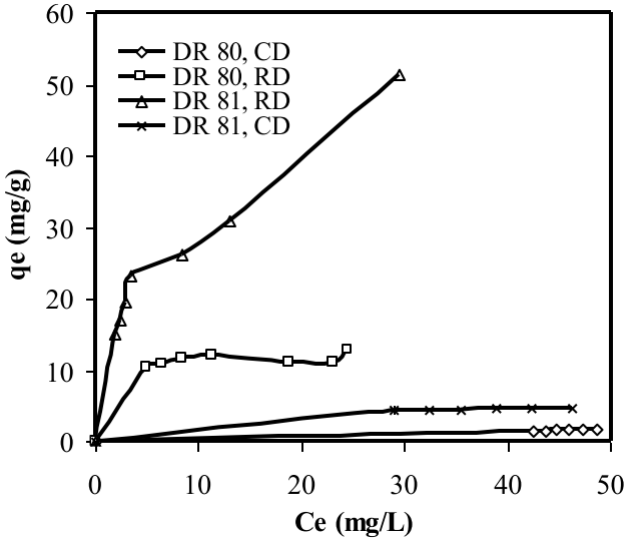

Fig. 15. Adsorption isotherms of DR 80 and DR 81 dyes onto RD and CD.

The values of K_L and Q_0 were calculated from the slope and intercept of the linear plot of $1/q_e$ against $1/Ce$.

Another isotherm model is the Freundlich model, which was also applied for the adsorption of DR 80 and DR 81 dyes on diatomite as given below:

$$q_e = K_F C_e^{\frac{1}{n}} \tag{2}$$

Where, Ce is the equilibrium dye concentration in the aqueous system (mg/L), q_e denotes the amount of dye adsorbed per weight of the adsorbent used (mg/g), K_F and n are the Freundlich isotherm constants depending on temperature and adsorbent-adsorbate system [40].

The Freundlich equation (Eq. [2]) can be linearised as follows:

$$\log_{10} q_e = \log_{10} K_F + \frac{1}{n} \log_{10} C_e \tag{3}$$

A linear plot of log10 q_e versus log10 Ce gives the values of K_F and n.

The Brunauer-Emmett-Teller (BET) model was also examined in this study to describe the adsorption equilibrium. A linear expression of the BET isotherm model may be written as:

$$\frac{C_e}{(C_s - C_e) q_e} = \frac{1}{K_b q_m} + \left(\frac{K_b - 1}{K_b q_m} \right) \left(\frac{C_e}{C_s} \right) \tag{4}$$

Where, Ce is the concentration of dye in solution (mg/L), Cs denotes the saturation concentration of dye (mg/L), q_e represents the amount of dye adsorbed per weight of the adsorbent used (mg/g), q_m refers to the amount of dye adsorbed in forming a complete monolayer (mg/g), K_b indicates a constant explaining the energy of interaction with the surface.

The values of K_b and q_m were calculated from the slope and intercept of the linear plot of $\left(\frac{C_e}{C_S - C_e}\right)\frac{1}{q_e}$ versus $\frac{C_e}{C_S}$.

The determined constants and the correlation coefficients of the Langmuir, Freundlich and BET isotherms are illustrated in Table 1. The negative values of Kb related to the BET isotherm model indicate that the adsorption process did not follow the BET isotherm model. It is evident from Table 1 that the isotherm data for the adsorption of DR 80 dye by RD were best-fitted to Langmuir model with a correlation coefficient of 0.977. Furthermore, the Freundlich model is most appropriate for the adsorption of DR 81 dye on RD with a correlation coefficient of 0.993. Table 1 also shows that the adsorption of both DR 80 and DR 81 dyes by CD can be well described by Freundlich isotherm model with the correlation coefficients of 0.965 and 0.947, respectively.

Table 1. Parameters of Langmuir, Freundlich and BET isotherms for adsorption of DR 80 and DR 81 dyes by RD and CD.

		Langmuir isotherm constants			Freundlich isotherm constant			BET isotherm constants		
Adsorbent	Dye	Q_0	K_L	R^2	K_F	$\frac{1}{n}$	R^2	K_b	q_m	R^2
RD	DR80	13.33	0.68	0.977	8.87	0.111	0.899	-3.67	0.021	0.9417
RD	DR81	40.0	0.33	0.957	12.6	0.35	0.993	-14.7	0.018	0.9704
CD	DR80	81.3	0.4×10^{-7}	0.964	0.041	0.49	0.965	- 0.16	0.05	0.827
CD	DR81	5.78	0.104	0.930	2.13	0.212	0.947	- 0.65	0.41	0.841

3.7. Adsorption kinetics

The prediction of the rate at which dye is removed from an aqueous system is an essential task in order to design a suitable treatment system based on an adsorption process. The kinetics data for the adsorption of DR 80 and DR 81 dyes by diatomite were treated with the pseudo-first-order Lagergren rate equation [3, 13, 16] and the pseudo-second-order rate expression developed by Ho and McKay [41]. The Lagergren equation can be expressed as:

$$\log(q_e - q_t) = \log q_e - \frac{K_{1,ad}}{2.303} t \quad (5)$$

Where, q_e and q_t refer to the amount of dye (*mg/g*) adsorbed at equilibrium and time t (min) and $K_{1,ad}$ is the pseudo-first-order rate constant (1/min).
The Ho and McKay rate equation is given by:

$$\frac{t}{q_t} = \frac{1}{K_{2,ad}\, q_e^{\,2}} + \frac{t}{q_e} \quad (6)$$

Where, q_e and q_t are the amounts of dye (*mg/g*) adsorbed at equilibrium and time t (min) and $K_{2,ad}$ represents the rate constant of the pseudo-second -order model (*g/mg* min).

Linear plot of log10 ($q_e - q_t$) against t gives the rate constant of $K_{1,ad}$. In addition, the value of $K_{2,ad}$ is obtained from the intercept of the linear plot of t/q_t versus t.

Adsorption kinetics constants of the pseudo-first-order and pseudo-second-order models at pH 2, temperature 25˚C, an agitation speed of 200 rpm, an initial concentration of 50 mg/L, and for a time period of 300 minutes are given in Table 2. It is clear from this table that the high values of correlation coefficients of the pseudo-second-order model for the adsorption of RD 80 and RD 81 dyes by both RD and CD indicate that the adsorption data conformed well to the Ho and McKay kinetics model.

Table 2. Kinetics constants for DR 80 and DR 81 dyes adsorption by RD and CD.

Adsorbent	Dye	Pseudo-first-order			Pseudo-second-order		
		q_1 (mg/g)	$K_{1,ad}$ (1/min)	R^2	q_e (mg/g)	$K_{2,ad}$ (g/mg min)	R^2
RD	DR 80	2.125	0.00622	0.9182	10.27	0.0405	0.9998
RD	DR 81	4.912	0.00668	0.7940	23.26	0.0202	0.9999
CD	DR 80	0.461	0.0094	0.6960	1.598	0.1930	0.9988
CD	DR 81	3.60	0.00329	0.9622	7.17	0.0163	0.9893

3.8. Effect of pH

The pH of the aqueous medium is an important variable for the adsorption of dyes on the solid particles of the adsorbents. pH studies were carried out to determine the optimum pH at which maximum colour removal could be achieved with diatomite for DR 80 and DR 81 dyes. The effect of pH on both dyes by diatomite was observed over a broad pH range of 2-12. The effect of pH on DR 80 and DR 81 dyes adsorption is shown in Fig. 16.

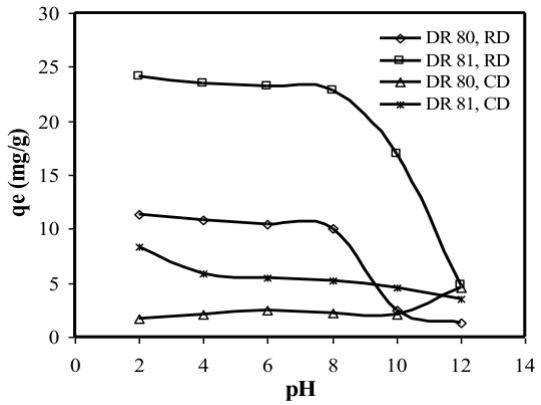

Fig. 16. Effect of pH on the adsorption of DR 80 and DR 81 dyes by RD and CD; Conditions: T=25 0C , agitation speed = 200 rpm, equilibrium time = 300 minutes.

Results show that for both RD and CD adsorbents, the optimum pH value for the adsorption of DR 80 and DR 81 dyes was pH 2. The dye adsorption by RD decreased steadily (from 11.40 to 10.10 mg/g for DR 80 dye and from 24.115 to 22.8 mg/g for DR 81 dye) as the solution pH was increased from 2 to 8. The amount of DR 81 dye sorbed decreased sharply from 22.8 to 4.87 mg/g when pH was raised from 8 to 12. Whereas, within pH 8 to 10, the DR 80 dye adsorption decreased sharply from 10.10 to 2.46 mg/g. It decreased again at a slower rate from 2.46 to 1.31 mg/g when pH was varied from 10 to 12.

The adsorption of DR 80 dye by CD increased slightly from 1.66 to 2.44 mg/g with increasing pH of dye solution from 2 to 6. But, in the pH range of 6-10, the amount of DR 80 dye sorbed on CD was somewhat decreased from 2.44 to 2.13 mg/g. Above pH 10 till pH 12 it increased linearly from 2.3 to 4.54 mg/g.

It is evident from Fig 16 that the quantity of DR 81 dye sorbed on CD decreased from 8.325 to 5.88 mg/g between pH 2 and 4. At pH values above 4 the adsorption of DR 81 dye by CD decreased again at a steady rate from 5.88 to 3.58 mg/g.

The maximum sorption capacity of RD occurred at pH 2 and the corresponding sorption capacities were 11.40 and 24.115 mg/g for DR 80 and DR 81 dyes, respectively, so the effective pH was 2 and it was used in all adsorption experiments.

Figs. 17 to 20 show the Ho and McKay linear plots obtained for various pHs ranging from 2 to 12. Figs. 17 and 18 refer to the adsorption of DR 80 dye by RD and CD, respectively. Figs. 19 and 20 are related to the adsorption of DR 81 dye by RD and CD, respectively.

The kinetics constants of the pseudo-first-order and pseudo-second-order models at different pHs are given in Tables 3 and 4 for DR 80 and DR 81 dyes adsorption, respectively. These parameters were obtained from the Lagergren and Ho and McKay plots. As illustrated well, at any pH and for both RD and CD, the high values of correlation coefficients show that the adsorption process follows the pseudo-second-order kinetic model.

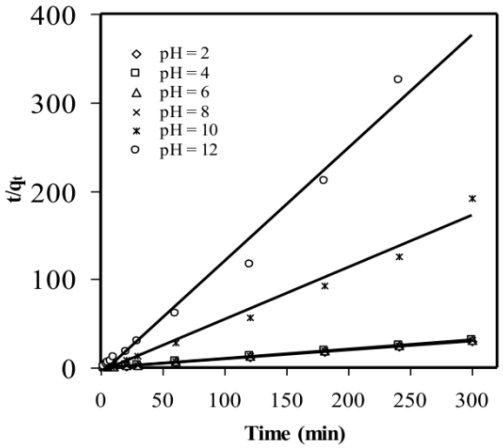

Fig. 17. Pseudo-second-order sorption kinetics of DR 80 dye onto RD at various pH; Conditions: agitation speed = 200 rpm, initial dye concentration = 50 mg/L, T=25˚C.

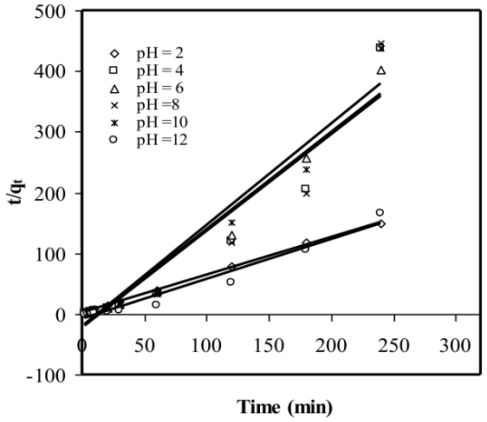

Fig. 18. Pseudo-second-order sorption kinetics of DR 80 dye onto CD at various pH; Conditions: agitation speed = 200 rpm, initial dye concentration = 50 mg/L, T=25˚C.

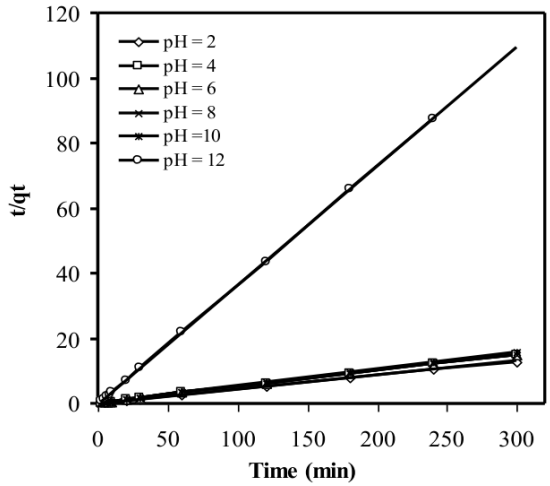

Fig. 19. Pseudo-second-order sorption kinetics of DR 81 dye onto RD at various pH; Conditions: agitation speed = 200 rpm, initial dye concentration = 50 mg/L, T=25˚C.

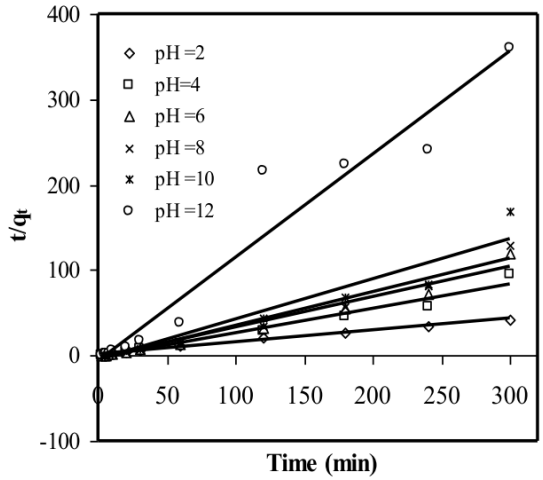

Fig. 20. Pseudo-second-order sorption kinetics of DR 81 dye onto CD at various pH; Conditions: agitation speed = 200 rpm, initial dye concentration = 50 mg/L, T=25˚C.

3.9. Effect of temperature

Temperature has a significant effect on the adsorption process. Increasing the temperature will change the equilibrium capacity of the adsorbent for a particular adsorbate. Furthermore, an increase in temperature can raise the rate of diffusion of the dye molecules in the internal pores of the adsorbent [20]. In this study, the removal of DR 80 and DR 81 dyes from aqueous solution using diatomite has been investigated at four different temperatures ranging from 25 to 55˚C. The Ho and McKay linear plots are shown in Figs. 21 to 24 for different temperatures and for both RD and CD. The kinetic parameters of adsorption at different temperatures are also given in Tables 5 and 6 for DR 80 and DR 81 dyes, respectively. It can be observed from Figs. 21 to 23, that at any temperature and for both RD and CD, the adsorption process follows the pseudo-second-order kinetic model. However, the adsorption of DR 81 dye on CD at a temperature 55˚C may follow the pseudo-first-order kinetics model. It is also evident from Figs. 21 to 24 the adsorption process increases with an increase in temperature.

Table 3. Kinetics constants of DR 80 dye adsorption onto RD and CD at different pH.

		pseudo-first-order kinetic constants			pseudo-second-order kinetic constants		
Adsorbent	pH	$K_{1,ad}$	q_e	R^2	$K_{2,ad}$	q_e	R^2
	2	0.00622	2.125	0.9182	0.0405	10.27	0.9998
	4	0.00530	2.782	0.8743	0.0324	9.452	0.9996
RD	6	0.00553	2. 798	0.9190	0.0295	9.590	0.9994
	8	0.00530	2.511	0.8750	0.0320	9.728	0.9995
	10	0.0051	- 0.185	0.7092	-0.0899	1.700	0.9825
	12	0.00161	-0.282	0.2193	-0.2360	0.784	0.9837
	2	0.00940	0.461	0.6960	0.1930	1.598	0.9988
	4	-0.0097	0.187	0.6581	-0.1150	0.629	0.9201
CD	6	-0.0064	0.510	0.3734	-0.1310	0.626	0.9654
	8	-0.0076	0.310	0.4101	-0.1150	0.625	0.9086
	10	-0.0081	0.300	0.6384	-0.1330	0.598	0.9537
	12	-0.0092	0.370	0.3409	-0.0533	1.530	0.9631

Table 4. Kinetics constants of DR 81 dye adsorption onto RD and CD at different pH.

		pseudo-first-order kinetic constants			pseudo-second-order kinetic constants		
Adsorbent	pH	$K_{1,ad}$	q_e	R^2	$K_{2,ad}$	q_e	R^2
	2	0.00668	4.912	0.794	0.0202	23.26	0.9999
	4	0.0025	7.880	0.8529	0.0181	19.96	0.9997
RD	6	0.0025	7.78	0.8687	0.0179	19.96	0.9996
	8	0.0028	7.31	0.8792	0.018	19.80	0.9996
	10	0.00021	8.041	0.8924	0.0196	19.08	0.9996
	12	0.00012	15.95	0.592	-1.442	2.737	0.9999
	2	0.00329	3.60	0.9622	0.0163	0. 7.17	0.9893
	4	-0.00370	0.867	0.6888	-0.0428	3.541	0.9721
CD	6	-0.00368	1.032	0.9047	- 0.0407	2.788	0.9706
	8	-0.00392	0.925	0.6131	- 0.0393	2.557	0.9688
	10	- 0.0035	1.107	0.8181	- 0.0430	2.10	0.9327
	12	- 0.0035	1.244	0.5615	- 0.285	0.831	0.9489

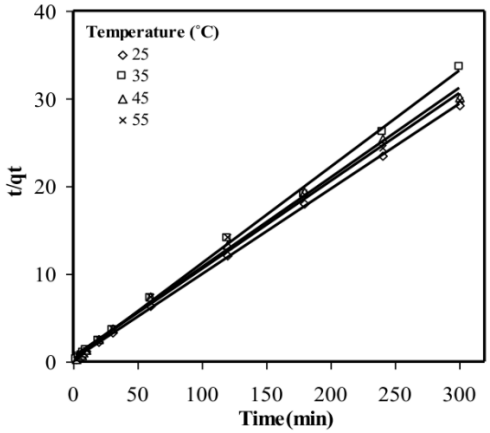

Fig. 21. Pseudo-second-order sorption kinetics of DR 80 dye onto RD at different temperatures; Conditions: agitation speed = 200 rpm, initial dye concentration = 50 mg/L, pH = 2.

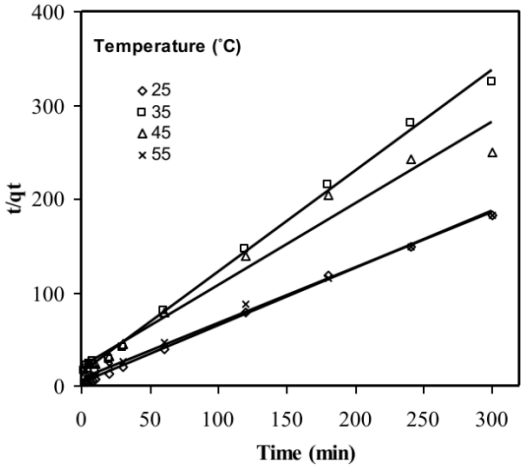

Fig. 22. Pseudo-second-order sorption kinetics of DR 80 dye onto CD at different temperatures; Conditions: agitation speed = 200 rpm, initial dye concentration = 50 mg/L, pH = 2.

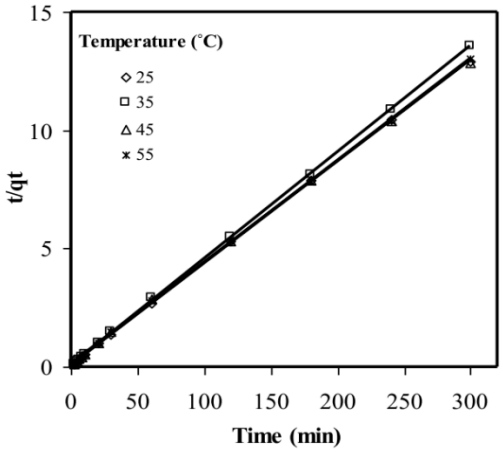

Fig. 23. Pseudo-second-order sorption kinetics of DR 81 dye onto RD at different temperatures; Conditions: agitation speed = 200 rpm, initial dye concentration = 50 mg/L, pH = 2.

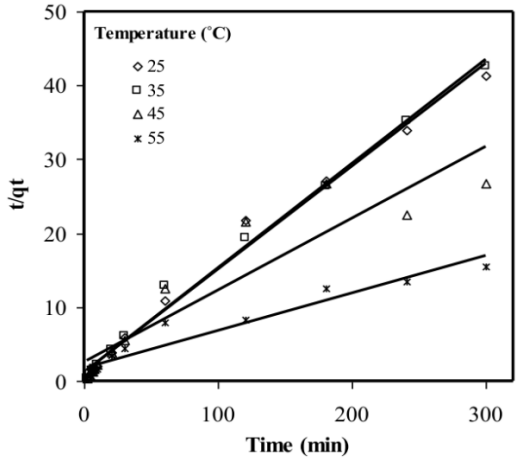

Fig. 24. Pseudo-second-order sorption kinetics of DR 81 dye onto CD at different temperatures; Conditions: agitation speed = 200 rpm, initial dye concentration = 50 mg/L, pH = 2.

Table 5. Kinetics constants of DR 80 dye adsorption onto RD and CD at different temperatures.

Adsorbent	T (^0C)	pseudo-first-order kinetic constants			pseudo-second-order kinetic constants		
		$K_{1,ad}$	q_e	R^2	$K_{2,ad}$	q_e	R^2
RD	25	0.0062	2.12	0.9182	0.041	10.27	0.9998
	35	0.0035	2.59	0.7236	0.049	9.11	0.9985
	45	0.0048	3.42	0.9717	0.02	9.79	0.9976
	55	0.00461	3.63	0.9733	0.01	9.97	0.9958
CD	25	0.0101	0.474	0.8215	0.151	1.632	0.9987
	35	0.0152	0.571	0.7876	0.084	0.930	0.9965
	45	0.00875	0.954	0.8344	0.0385	1.143	0.9750
	55	0.0106	1.033	0.9736	0.0436	1.686	0.9971

Table 6. Kinetics constants of DR 81 dye adsorption onto RD and CD at different temperatures.

Adsorbent	T (^0C)	pseudo-first-order kinetic constants			pseudo-second-order kinetic constants		
		$K_{1,ad}$	q_e	R^2	$K_{2,ad}$	q_e	R^2
RD	25	0.0067	4.91	0.6913	0.0203	23.26	0.9999
	35	0.0044	4.81	0.8258	0.0247	22.22	0.9999
	45	0.0120	5.40	0.7320	0.0140	23.42	0.9997
	55	0.0067	5.25	0.8668	0.0114	23.26	0.9998
CD	25	0.00392	3.60	0.9622	0.0163	7.168	0.9893
	35	0.00069	14.20	0.9269	0.0159	7.077	0.9933
	45	0.00115	16.05	0.9043	0.0062	8.710	0.9369
	55	0.0060	17.73	0.9729	0.00144	19.960	0.9308

4. Conclusions

Diatomite has been studied for the removal of DR 80 and DR 81 dyes from a synthetic aqueous solution. The functional groups of these dyes are almost similar, but the molecular size of DR 80 is two times greater than that of DR 81. Thermal treatment of the adsorbent at 980˚C adversely affected the adsorption process due to the reduction of the volume of the pore spaces, specific surface area and removal of the surface functional groups from the RD. The adsorption process was also influenced by solution pH and temperature. The maximum sorption capacity of RD occurred at pH 2 and the corresponding sorption capacities were 11.40 and 24.115 mg/g for DR 80 and DR 81 dyes, respectively. The adsorption of DR 80 and DR 81 dyes by diatomite increased with an increase in temperature. Equilibrium data for the adsorption of DR 80 and DR 81 dyes by RD fit well to the Langmuir and Freundlich isotherm models, respectively. Furthermore, the Freundlich model is most appropriate for the adsorption of DR 80 and DR 81 dyes on CD. In addition, the rate of adsorption process obeys the pseudo-second-order kinetics model. In order to obtain the highest possible removal of DR 80 and DR 81 dyes, the experiments were carried out at pH 2, temperature 25˚C, an agitation speed of 200 rpm, an initial dye concentration of 50 mg/L, a centrifugal rate of 4000 rpm and a process time of 300 minutes. Under these conditions, a maximum percentage removal of 90.19 and 93.08 % were therefore obtained for DR 80 and DR 81 dyes from an aqueous solution using RD.

The experimental results illustrate that both investigated steps of adsorption, including diffusion and adsorption on surfaces steps are important, but the size of dye molecule is more effective, especially on the adsorption capacity of the adsorbent. It means that diffusion through the micro-pores is the most important step
of the adsorption mechanism and adsorption on the adsorbent surfaces has the second place of significance.

Acknowledgments

The authors are thankful to Institute for Color Science and Technology (ICST) for providing the financial help and to Shahrood University of Technology, for supporting this research.

Ethical Considerations

The authors avoided data fabrication, falsification, and plagiarism, and any form of misconduct.

Funding

This research did not receive any specific grant from funding agencies in the public, commercial, or not-for-profit sectors.

Conflict of Interest

The authors declare no conflict of interest.

References

[1] Uddin, F. (2021). Environmental hazard in textile dyeing wastewater from local textile industry. *Cellulose*, 28(15): 10715-10739. https://doi.org/10.1007/s10570-021-04228-4

[2] Mani, S., Chowdhary, p., Bharagva, R.N. (2019). Textile Wastewater Dyes: Toxicity Profile and Treatment Approaches, in Emerging and Eco-Frendly Approaches for Waste Management. Springer, Singapore, pp. 219-244. https://doi.org/10.1007/978-981-10-8669-4_11

[3] Gong, R., Ding, Y., Li, M., Yang, C., Liu, H., Sun, Y. (2005). Utilization of powdered peanut hull as biosorbent for removal of anionic dyes from aqueous solution. *Dyes and Pigments*, 64(3): 187-192. https://doi.org/10.1016/j.dyepig.2004.05.05

[4] Khraisheh, M.A.M., Al-Ghouti, M.A., Allen, S.J., Ahmad, M.N. (2005). Effect of OH and silanol groups in the removal of dyes from aqueous solution using diatomite. *Water Research*, 39(5): 922-932. https://doi.org/10.1016/j.watres.2004.12.008

[5] Venkata Mohan, S., Sailaja, P., Srimurali, M., Karthikeyan, J. (1999). Color removal of monoazo acid dye from aqueous solution by adsorption and chemical coagulation. *Environmental Engineering and Policy*, 1:149-154. https://doi.org/10.1007/s100220050016

[6] Panswed, J., Wongchaisuwan, S. (1986). Mechanism of dye wastewater color removal by magnesium carbonate-hydrated basic. *Water Science and Technology*, 18: 139-144. https://doi.org/10.2166/wst.1986.0045

[7] Chun, H., Yizhong, W. (1999). Decolorization and biodegradability of photocatalytic treated azo dyes and wool textile wastewater. *Chemosphere*, 39(12): 2107-2115. https://doi.org/10.1016/S0045-6535(99)00118-6

[8] Hachem, C., Bocquillon, F., Zahraa, O., Bouchy, M. (2001). Decolourization of textile industry wastewater by the photocatalytic degradation process. Dyes and Pigments, 49(2): 117-125. https://doi.org/10.1016/S0143-7208(01)00014-6

[9] Daneshvar, N., Behnajady, M.A., Khayyat, Ali Mohammadi, M., Seyed Dorraji M.S. (2008). UV/H2O2 treatment of Rhodamine B in aqueous solution: Influence of operational parameters and kinetic modeling. *Desalination*, 230(1-3): 16-26. https://doi.org/10.1016/j.desal.2007.11.012

[10] Wu, J., Eiteman, M.A., Law, S.E. (1998). Evaluation of membrane filtration and ozonation processes for treatment of reactive dye wastewater. *Journal of Environmental Engineering*, 124(3): 272-277. https://doi.org/10.1061/(ASCE)0733-9372(1998)124:3(272)

[11] Pearce, C.L., Lloyd, J.R., Guthrie, J.T. (2003). The removal of colour from textile wastewater using whole bacterial cells: a review. *Dyes and Pigments*, 58(3): 179-196. https://doi.org/10.1016/S0143-7208(03)00064-0

[12] Vlyssides, A.G., Loizidou, M., Karlis, P.K., Zorpas, A.A., Papaioannou, D. (1999). Electrochemical oxidation of a textile dye wastewater using a Pt/Ti electrode. *Journal of Hazardous Materials*, 70(1-2): 41-52. https://doi.org/10.1016/S0304-3894(99)00130-2

[13] Fu, Y., Viraraghavan, T. (2002). Removal of congo red from an aqueous solution by fungus Aspergillus niger. *Advances in Environmental Research*, 7(1): 239-247. https://doi.org/10.1016/S1093-0191(01)00123-X
[14] Doulati Ardejani, F., Badii, Kh., Yousefi Limaee, N., Shafaei, S.Z., Mirhabibi, A.R. (2008). Adsorption of Direct Red 80 dye from aqueous solution onto almond shells: Effect of pH, initial concentration and shell type. *Journal of Hazardous Materials*, 151 (2-3): 730-737. https://doi.org/10.1016/j.jhazmat.2007.06.048
[15] Gucek, A., Sener, S., Bilgen, S., Mazmanci, M.L. (2005). Adsorption and kinetic studies of cationic and anionic dyes on pyrophyllite from aqueous solutions. Gucek A., Sener S., Bilgen S., Mazmanci M.L. (2005). Adsorption and kinetic studies of cationic and anionic dyes on pyrophyllite from aqueous solutions. *Journal of Colloid and Interface Science*, 286(1): 53-60. https://doi.org/10.1016/j.jcis.2005.01.012
[16] Namasivayam, C., Arasi, D.J.S.E. (1997). Removal of congo red from wastewater by adsorption onto waste red mud. *Chemosphere*, 34(2): 401-417. https://doi.org/10.1016/S0045-6535(96)00385-2
[17] Netpradit, S., Thiravetyan, P., Towprayoon, S. (2004). Adsorption o three azo reactive dyes by metal hydroxide sludge: effect of temperature, pH, and electrolytes. *Journal of Colloid and Interface Science*, 270(2): 255-261. https://doi.org/10.1016/j.jcis.2003.08.073
[18] Norouzi, Sh., Badii, Kh., Doulati Ardejani, F. (2010). Activated bauxite waste as an adsorbent for removal of Acid Blue 92 from aqueous solutions. *Water Science and Technology*, 62(11): 2491-2500. https://doi.org/10.2166/wst.2010.514
[19] Pala, A., Tokat, E. (2002). Color removal from cotton textile industry wastewater in an activated sludge system with various additives. *Water Research*, 36(11): 2920-2925. https://doi.org/10.1016/S0043-1354(01)00529-2
[20] Wang, S., Boyjoo, Y., Choueib, A., Zhu, Z.H. (2005). Removal of dyes from aqueous solution using fly ash and red mud. *Water Research*, 39(1): 129-138. https://doi.org/10.1016/j.watres.2004.09.011
[21] Game, P.S. (2022). Some Polyaniline Based Adsorbent materials for the Removal of dyes and Heavy Metals from Solution: A Review. *International Journal of Creative Research Thoughts*, 10(2): 89-95.
[22] Li, R., Tang, X., Wu, J., Zhang, K., Zhang, Q., Wang, J., Zheng, J., Zheng, S., Fan, J., Zhang, W., Li, X., Cai, S. (2023). A sulfonate-functionalized covalent organic framework for record-high adsorption and effective separation of organic dyes. *Chemical Engineering Journal*, 464, 142706. http://dx.doi.org/10.2139/ssrn.4358165
[23] Aggarwal, R., Garg, A. K., Saini, D., Sonkar, S. K., Sonker, A. K., Westman, G. (2023). Cellulose Nanocrystals Derived from Microcrystalline Cellulose for Selective Removal of Janus Green Azo Dye. *Industrial & Engineering Chemistry Research*, 62(1), 649–659. https://doi.org/10.1021/acs.iecr.2c03365
[24] Aksu, Z. (2005). Application of biosorption for the removal of orange pollutants: a review. *Process Biochemistry*, 40(3-4): 997-1026. https://doi.org/10.1016/j.procbio.2004.04.008
[25] Garg, V.K., Gupta, R., Yadav, A.B., Kumar, R. (2003). Dye removal from aqueous solution by adsorption on treated sawdust. *Bioresources Technology*, 89(2): 121-124. https://doi.org/10.1016/S0960-8524(03)00058-0
[26] Garg, V.K., Amita, M., Kumar, R., Gupta, R. (2004). Basic dye (methylene blue) removal from simulated wastewater by adsorption using Indian Rosewood sawdust: a timber industry waste. *Dyes and Pigments*, 63(3): 243-250. https://doi.org/10.1016/j.dyepig.2004.03.005
[27] Pavel, J., Buchtova, H., Ryznarova, M. (2003). Sorption of dyes from aqueous solutions onto fly ash. *Water Research*, 37(20): 4938-4944. https://doi.org/10.1016/j.watres.2003.08.011
[28] Robinson, T., Chandra, B., Nigam, P. (2002). Removal of dyes from a synthetic textile dye effluent by biosorption on apple pomace and wheat straw. *Water Research*, 36(11): 2824-2830. https://doi.org/10.1016/s0043-1354(01)00521-8
[29] Doulati Ardejani, F., Badii, Kh., Yousefi Limaee, N., Mahmoodi, N.M., Arami, M., Shafaei, S.Z., Mirhabibi, A.R. (2007). Numerical modelling and laboratory studies on the removal of Direct Red 23

and Direct Red 80 dyes from textile effluents using orange peel, a low-cost adsorbent. *Dyes and Pigments*, 73(2): 178-185. https://doi.org/10.1016/j.dyepig.2005.11.011

[30] Namasivayam, C., Muniasamy, N., Gayatri, K., Ran,i M., Ranganathan, K. (1996). Removal of dyes from aqueous solutions by cellulosic waste orange peel. *Bioresources Technology*, 57(1): 37-43. https://doi.org/10.1016/0960-8524(96)00044-2

[31] Annadurai, G, Juang, R.S., Lee, D.J. (2002). Use of cellulose-based wastes for adsorption of dyes from aqueous solutions. *Journal of Hazardous Materials*, 92(3): 263-274. https://doi.org/10.1016/S0304-3894(02)00017-1

[32] Bhattacharyya, K.G., Sarma, A. (2003). Adsorption characteristics of the dye, brilliant green, on neem leaf powder. *Dyes and Pigments*, 57(3): 211-222. https://doi.org/10.1016/S0143-7208(03)00009-3

[33] Sriram, G., Kigga, M., Uthappa, U.T., Rego, R. M., Thendral, V., Kumeria, T., Jung, H-Y., Kurkuri, M. D. (2020). Naturally available diatomite and their surface modification for the removal of hazardous dye and metal ions: a review. *Advances in Colloid and Interface Science*, 282, 102198. https://doi.org/10.1016/j.cis.2020.102198

[34] Al-Ghouti M., Khraisheh M.A.M., Ahmad M.N.M., Allen S. (2005). Thermodynamic behaviour and the effect of temperature on the removal of dyes from aqueous solution using modified diatomite: A kinetic study. *Journal of Colloid and Interface Science*, 287(1): 6-13. https://doi.org/10.1016/j.jcis.2005.02.002

[35] Erdem E, Çölgeçen G, Donat R. (2005). The removal of textile dyes by diatomite earth. *Journal of Colloid and Interface Science*, 282(2): 314-319. https://doi.org/10.1016/j.jcis.2004.08.166

[36] Badii Kh., Doulati Ardejani F., Aziz Saberi M., Yousefi Limaee N., Shafaei S.Z. (2010). Adsorption of Acid blue 25 dye on diatomite in aqueous solutions. *Indian Journal of Chemical Technology*, 17: 7-16.

[37] Al-Ghouti M.A., Li J., Salamh Y., Al-Laqtah N., Walker G., Ahmad M.N.M. (2010). Adsorption mechanisms of removing heavy metals and dyes from aqueous solution using date pits solid adsorbent, *Journal of Hazardous Materials*, 176(1-3): 510-520. https://doi.org/10.1016/j.jhazmat.2009.11.059

[38] Yuan, W., Li, M., Chen, H., Liu, G., Liu, D., Chen, X., Song, W., Su, Y (2024). Preparation of porous CuS/modified-diatomite composite via a facile in situ loading process for efficient recovery of silver ion from aqueous solution. *Applied Surface Science*, 644, 158753. https://doi.org/10.1016/j.apsusc.2023.158753

[39] Asatekin A., Mayes, A.M. (2009). Amphiphilic graft copolymers for nanofiltration membranes with tunable pore size. 2.500 Desalination and Water Purification, MIT Open Courseware, http://ocw.mit.edu.

[40] Gokmen V., Serpen A. (2002). Equilibrium and kinetic studies on the adsorption of dark colored compounds from apple juice using adsorbent resin. *Journal of Food Engineering*, 53(3): 221-227. https://doi.org/10.1016/S0260-8774(01)00160-1

[41] Karaca S., Gurses A., Bayrak R. (2005). Investigation of applicability of the various adsorption models of methylene blue adsorption onto lignite/water interface. *Energy Conversion and Management*, 46(1): 33-46. https://doi.org/10.1016/j.enconman.2004.02.008